Available online at www.sciencedirect.com
SCIENCE DIRECT
Optics Communications 260 (2006) 324–328
OPTICS COMMUNICATIONS
www.elsevier.com/locate/optcom

High accuracy measurement of the residual air gap thickness of thin-film and solid-spaced filters assembled by optical contacting

Johan Floriot, Fabien Lemarchand *, Laetitia Abel-Tiberini, Michel Lequime

Institut Fresnel, UMR CNRS 6133, Université Paul Cézanne, Domaine Universitaire de Saint-Jérôme, 13397 Marseille, Cedex 20, France

Received 27 April 2005; received in revised form 31 August 2005; accepted 5 October 2005

Abstract

Optical contacting is a powerful tool for assembling solid-spaced filters in order to form a wavelength division multiplexing (WDM) multiple-cavity filter. In this article, we propose a method able to characterize the optical quality of such assembling with a high accuracy. We use localized spectral transmittance measurements to map the thickness of the residual air gap existing at the adhesion interface with a few nanometers precision. Tests on thick (2 mm) and thin (100 μm) substrates coated by Dual Ion Beam Sputtering are performed. Thus, we show that our 25 mm-diameter samples are strictly contacted over more than 80% of their surface, with no detectable residual air gap.

PACS: 68.55.−a; 68.55.Jk; 78.66.−w; 77.55.+f; 42.79.Wc; 81.15.Cd

1. Introduction

To fulfill WDM requirements, thin-film filters including a very high number of layers (more than one hundred) should be considered. This great number of layers can be drastically reduced by the use of solid-spaced filters [1–3]. We showed [4] that, following this alternative approach, it is relatively easy to manufacture WDM filters for multiplexing/demultiplexing and add/drop applications. The method is based on the use of high quality thin substrates coated on both sides with few layers. Passive [5] and tunable [6] multiple-cavity filters using air gap as coupling layer have been achieved. Nevertheless, in order to satisfy the use constraints of WDM components, it is naturally critical to achieve the assembly of such filters in a rugged and compact way. The use of epoxy cement on the light path is strongly prohibited by WDM standards because of aging. As a consequence, we chose to directly assemble our filters by optical contacting. This well-known assembling technique is widely used in optoelectronics [7] (heterojunctions) and massive optics [8] (Fabry–Perot etalons, cube beamsplitters). The adhesion arises through intermolecular attraction, when two high-optical-quality surfaces are put in close contact [9–11], and generally, this kind of assembling is nearly irreversible. This method has been proposed thirty years ago by Austin to adhere multilayer filters [2] but the complexity of the process was prohibitive for industrial applications. Moreover, the checking of the quality of this adhesion, directly connected to the residual thickness of the air gap, is very often limited to a visual control with the observation of the disappearance of colored air gap fringes.

In this paper, we propose an experimental method to quantify with a great accuracy the quality of this adhesion. Spectral transmission of components assembled by optical contacting is measured with a high spatial and spectral resolution. From these measurements, the residual air gap thickness (RAGT) located at the interface of adhesion can be deduced with a high precision (few nanometers) and thus, RAGT mappings can be easily achieved. The highest precision should be obtained with a bonding

* Corresponding author. Tel.: +33 04 91 28 83 27; fax: +33 04 91 28 80 67.
E-mail address: fabien.lemarchand@frensnel.fr (F. Lemarchand).

0030-4018/$ - see front matter © 2005 Elsevier B.V. All rights reserved.
doi:10.1016/j.optcom.2005.10.015

located at a Fabry–Perot cavity spacer layer. Nonetheless, in order to manufacture high-optical-quality components with the highest maximum of transmittance and low scattering losses, we have deliberately made the choice to localize the adherence interface on the less sensitive layers of coating assembly, namely the coupling layer of a double-cavity Fabry–Perot filters.

2. Characterization of adhesion's optical quality between two coated thick substrates

All the coatings are manufactured with Dual Ion Beam Sputtering (DIBS) technology. In order to characterize adhesion on thick (2 mm) multilayer coated silica substrates, we use a spectrophotometric setup providing localized spectral transmission measurements described in a previous communication [12]. At the entrance, the system is illuminated by a quartz–halogen light source coupled in a 200 μm diameter core optical fibre. At the output, the spectral analysis is performed by an optical spectrum analyzer operating from 500 to 800 nm. The sample is placed in between, as well as a set of calibrated apertures that are imaged on the sample surface without magnification in order to select the diameter of the measured area (600 μm for our specific measurements). The spectral resolution is fixed to 0.5 nm, according to the diameter of the optical fibre that is connected to the spectrum analyser and which plays the role of the entrance slit of the monochromator.

The silica substrates of our contacting tests present the following specifications: 25 mm-diameter, 2 mm-thickness, $\lambda/10$ polishing ($\lambda = 633$ nm) and 0.5 nm-RMS roughness. An initial test between two cleaned bare substrates shows that the adhesion is effective on the whole contact surface. In the same way, the adhesion between one bare substrate and one substrate coated with five (Ta_2O_5/SiO_2) layers has been successfully achieved.

The most significant test consists in the adhesion of two simple-cavity multilayer filters in order to form a double-cavity one. We deposit on two substrates a bandpass filter [substrate/$H(LH)^3$ 4L $(HL)^3H$ 0.5L/air] centered at 630 nm. H is a high-index-quarter-wave layer (Ta_2O_5) and L is a low-index-quarter-wave layer (SiO_2). Each coating is ended with a 0.5L layer to simulate a final 1L coupling layer between both filters after contacting. Rear faces of both substrates remain uncoated. Deposition of each layer is controlled with an optical monitoring, (except the final 0.5L one) which ensures a good spectral positioning of the transmission window. After assembling, the final component, named filter A (see Fig. 1(a)), should present the spectral characteristics of an embedded double-cavity filter. To avoid dust contamination, no characterization has been performed between coating and assembling. A visual check allows us to suppose that the optical contacting (without any air gap) is achieved in the central area. Moreover, the adhesion is effective as the component withstands basic wrenching tests, annealing, and thermal shocks.

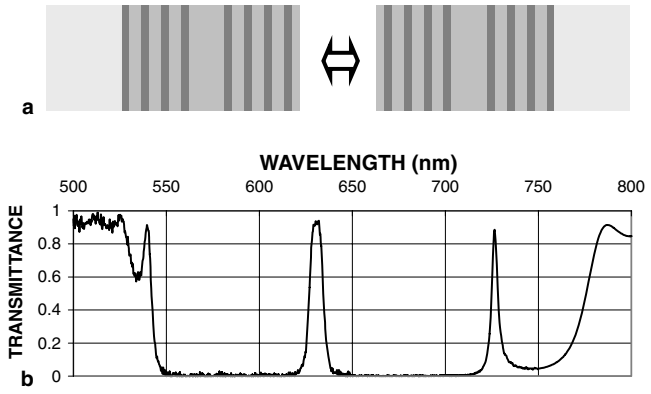

Fig. 1. (a) Design of filter A: substrate/$H(LH)^3$ 4L $(HL)^3H$ 0.5L – adhesion – 0.5L $H(LH)^3$ 4L $(HL)^3H$/substrate. (b) Experimental transmission in the contact area (central position of the incoming spot).

Using the measurement protocol above described, we obtain the transmission spectrum at the center of the surface of the sample (see Fig. 1(b)). We can observe that the transmitted peak around 630 nm reaches 92% which is very close to the theoretical value, as both substrates are not anti-reflecting coated on rear side. Thus, the contact procedure did not induce any scattering or absorbing losses and the filter has nearly optimal performances. The spectrum also presents a secondary peak located around 727 nm. Considering this coating technology, the real part of the refractive index of the H-material is estimated to 2.13 ± 0.01 in the wavelength range of analysis, whereas the refractive of B-material is estimated to 1.495 ± 0.005. The spectral interval between the two transmitted peaks (97 nm) is ten percent lower than the theoretical one considering design of filter A even when taking into account refractive index dispersion. A residual air gap between the two 0.5L layers would lead to increase the spectral interval and so cannot explain this difference. However, a deposition error on the two last coated layers (0.4L instead of 0.5L) can justify the spectrum of Fig. 1(b), and especially the location of the secondary peak at 727 nm. Such error is not unlikely as an inaccurate time monitoring has been used for this specific final layer.

When we scan different points at the surface of filter A, we can observe a slight spectral shift of the two transmitted peaks. The shift is more pronounced for the secondary peak. Several effects can contribute to these variations, like spectral drifts of the experimental setup, a non-uniformity of the performed coatings or the presence of a residual and inhomogeneous air gap at the adhesion interface. The spectral reproducibility of our setup is better than 0.1 nm: it allows excluding such a contribution. Vacuum chamber uniformity has been preliminary characterized for both SiO_2 and Ta_2O_5 single layers with the set up described in [12]. Considering filter A structure, major contribution of possible non-uniformity comes from SiO_2. The coating uniformity mapping presents smooth variations (valley shape) with a peak to valley relative shift of $\Delta t/t = 2 \times 10^{-3}$ along a 20 mm distance. This value corresponds to a maximum of

1.5 nm wavelength shift of filter A transmitted peaks. As a consequence, we will fix the precision of our measurement setup to the value corresponding to a spectral shift of 1.5 nm on both transmitted peaks. A lower measured shift could come from either a non-uniformity problem or a residual air gap.

Anyway, the resulting effect of a coating non-uniformity is characterized by a slow and continuous variation of the centering of the peaks with respect to the position of the spot at the surface of the sample: it is in complete contradiction with our observations: the spectral response around the secondary peak (and even around the principal one) over one diameter of filter A shows very slow then abrupt variations concerning the centering of the peak, as we will see below on RAGT determination curves.

Theoretically, both transmission peaks linearly shift towards higher wavelengths when the RAGT increases. The theoretical wavelength shifts are, respectively, 30 pm (principal peak) and 300 pm (secondary peak) for a RAGT change of 1 nm. Hence, it is more judicious to deduce the RAGT value from measured spectral data selected only around the secondary transmitted peak. The precision of the air gap thickness determination is hence about 5 nm considering a spectral shift of 1.5 nm of the secondary peak.

We use a standard least-square optimization method between theoretical calculation of the transmittance, function of an eventual air gap thickness t, and localized measurements of the spectral transmittance of filter A. We introduce a merit function MF defined by:

$$MF(t) = \frac{1}{N}\sqrt{\sum_{i=1}^{N}[T_{\exp}(\lambda_i) - T_{\text{th}}(\lambda_i, t)]^2},$$

where N is the number of considered data in the selected spectral interval, $T_{\exp}(\lambda)$ and $T_{\text{th}}(\lambda, t)$ are, respectively, the experimental and theoretical transmissions at wavelength λ. The theoretical transmission corresponds to a uniform design of filter A with a central zone 0.4L/air (thickness t)/0.4L. We restrict the wavelength range to (700–750 nm) (i.e., around the secondary peak). Under these considerations, the RAGT of filter A is equal to the thickness t corresponding to the minimum of MF. Experimental transmittance uncertainties can affect the RAGT determination. Repeatability tests enable to check the robustness of the procedure. We determine more than ten times the RAGT for a fixed single scanning zone, and deduce the precision of repeatability tests to about one nanometer, whereas the intrinsic precision of 5 nm.

We follow this procedure on filter A through different sections. The scanning points are 1 mm spaced. As an example, Fig. 2 represents deduced RAGT in the (0–45 nm) range for four different sections of filter A. Measurements performed through other scanning points show that the contact area (RAGT close to zero) approximately corresponds to 85% of the surface. It can reach several hundreds of nanometers in the non-contacted zone. The presence of this zone is probably due to internal stresses

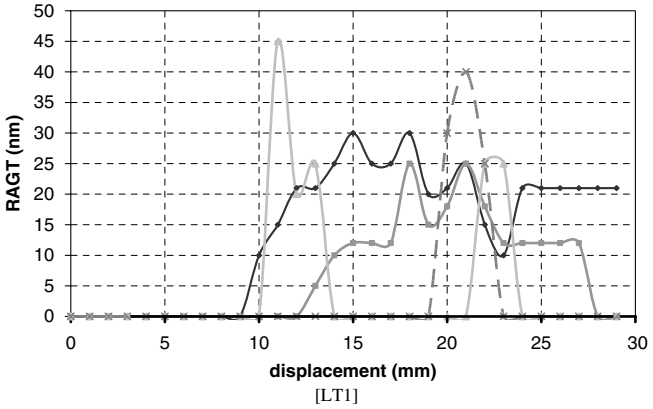

Fig. 2. RAGT determination for four different sections of filter A.

(substrate-intrinsic and coating-induced stresses). Small non-contacted spots exist too, with elementary surface about 1 mm^2. They can be associated to the presence of residual dusts or local coating defects. The changing shapes of the different RAGT curves confirm the hypothesis that coating uniformity is not the major cause of the spectral response shift.

3. Mapping of the residual air gap thickness between two bonded solid-spaced filters

In this part, thin silica substrates (100 μm-thick) are considered. We use the same cleaning and contacting procedure as for thick substrates. Solid-spaced filters (SSF) include substrates acting as Fabry–Perot spacers and induce very sharp transmitted peaks. Using such structures enables to neglect the coating non-uniformity phenomenon since the location of the peaks only depends on the solid spacer thickness. The spacer parallelism is quite excellent, measured to 3″. A high resolving characterization system [13] is necessary. The illumination of the sample is performed with a collimated beam coming from an EXFO tunable laser and the transmitted optical power is acquired with an InGaAs PIN photodiode followed by a low noise current-to-voltage converter-amplifier and a 16-bit analog to digital converter. The variations of this transmitted power are recorded by a computer during the laser sweep between 1520 and 1570 nm. A moving pinhole of 500 μm-diameter is used to localize the measurement at the surface of the sample. From laser characteristics, the spectral accuracy of the system is equal to 20 pm. In order to increase this accuracy, the monitor output of the tunable source is launched towards a reference set-up which includes a sealed air-spaced Fabry–Perot etalon with a constant free spectral range of 100 GHz and a thermal stability of about 10 pm/°C. The recording of the spectral transmittance function of this ASFPE is used to calibrate the wavelength scale of each laser scan with accuracy better than 10 pm.

Nonetheless, intermittently acquired spectra over a fixed zone on a resonant filter show a reproducibility of about 6 pm.

As an initial test, the adhesion of a thin bare substrate with a thick bare one is successfully done. The contacting of two thin bare substrates is also achieved.

The adhesion of two simple-cavity SSF is the most significant test. We also use DIBS technology with Ta_2O_5/SiO_2 coatings. The monitoring wavelength is fixed to 1550 nm. Thanks to transmittance characterizations, we first measure the optical thickness of two thin bare substrates. The spectral location of the transmission peaks is essentially given by the thickness of the cavities. We determine the silica thickness we need to deposit on the thinnest substrate to obtain identical optical thicknesses for the two solid spacers. After the preliminary SiO_2 deposition, the substrates are both-sided coated with a 7-layer dielectric mirror. A 0.5L layer is deposited at the end of one side coating. Hence, the design of each elementary solid-spaced filter is Air/$H(LH)^3$-cavity-$(HL)^3H$ 0.5L/Air. The adhesion process is performed at the middle of the L coupling layer. Once more no characterization has been performed before contacting to avoid contamination. After assembling, we obtain a double-cavity solid-spaced filter named filter B (see Fig. 3(a)). We have plotted on Fig. 3(b) the spectral transmittance experimentally recorded between 1549 and 1551 nm when the incoming spot is located at different positions on the sample surface. The transmission maximum is about 93% and variations of the centering of the peak are in the (0;50 pm) range. Other harmonic peaks present similar results.

Theoretical calculations show that the wavelength shifts of the transmitted peaks are all equal to 0.6 pm when the change of the RAGT is 1 nm. The low sensitivity of this kind of filter versus RAGT is in accordance with the fact that solid-spaced filters are one order of magnitude less sensitive to coating errors than thin-film filters [5]. The RAGT determination is performed following the same procedure as described before with a merit function taking into account data between 1549 and 1551 nm.

The precision of the RAGT evaluation corresponds to a 10 pm shift and is about 16 nm. The scan of the surface of

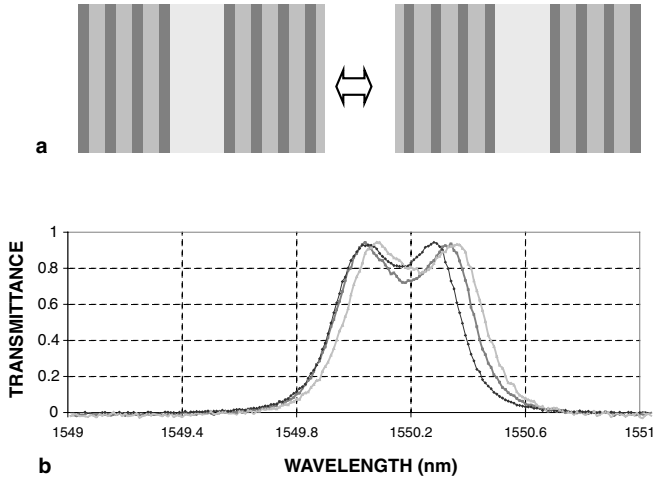

Fig. 3. (a) Design of filter B: $H(LH)^3$/substrate/$(HL)^3H$ 0.5L – adhesion – 0.5L $H(LH)^3$/substrate/$(HL)^3H$. (b) Experimental transmittance in the contact area for three different positions of the incoming spot.

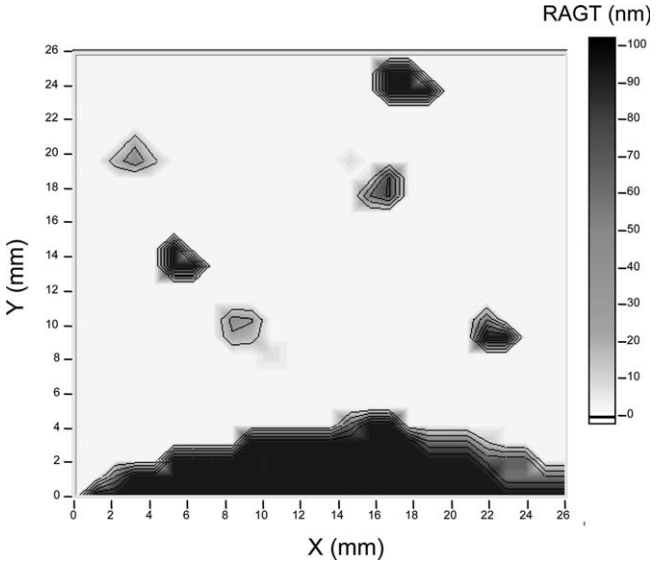

Fig. 4. RAGT mapping of filter B.

the filter B is performed with a spatial resolution of 1 mm. Fig. 4 is a mapping of the RAGT in the (0–100 nm) range. The filter is contacted on approximately 80% of the surface. Some small clusters with an RAGT of a few tens of nanometers are visible.

4. Conclusion

In this letter, we analyze the RAGT of double-cavity thin-film and solid-spaced filters assembled by optical contacting. With such components, compactness and solidity can be achieved and WDM miniaturization requirements are fulfilled. Our experimental characterizations allow us to check the value of the RAGT with a high precision by performing a fit between measured and theoretical transmittance. We then demonstrate that no interlayer exists when the adhesion of two samples is obtained. But, due to coating imperfections, dusts presence and internal stresses, non-contacted areas can exist with dimensions between one and several millimeters.

Technological developments are needed to achieve the adhesion over 100% of the contact surface. Moreover, in the perspective of thermally-tunable filters [6], the study of thermal behavior of contacted filters is very important. No effect is quantifiable on our preliminary tests including annealing (3 h at 300 °C) and thermal shocks (ambient to 100 °C). In addition, we note that the adhesion is always effective after storage (in air) during few months. A long-term study concerning aging and thermal behavior (annealing cycles, fatigue effects…) and quantization of the mechanical resistance remain to be achieved.

Acknowledgements

The authors thank J.J Fermé and J.M Combes from SESO (Société Européenne de Systèmes Optiques) for their

constructive remarks and for performing the adhesion process.

References

[1] J.A. Dobrowolski, J. Opt. Soc. Am. 49 (1959) 794.
[2] R.R. Austin, Opt. Eng. 11 (1972) 68.
[3] A.E. Roche, A.M. Title, Appl. Opt. 14 (1975) 765.
[4] J. Floriot, F. Lemarchand, M. Lequime, Opt. Commun. 222 (2003) 101.
[5] J. Floriot, F. Lemarchand, M. Lequime, Cascaded solid-spaced filters for DWDM applications, in: C. Amra, N. Kaiser, H.A. Macleod (Eds.), Advances in Optical Thin-Films, Proc. SPIE 5250 (2003) 384.
[6] J. Floriot, F. Lemarchand, M. Lequime, Opt. Exp. 12 (2004) 6289.
[7] H. Wada, H. Sasaki, T. Kamijoh, Solid-State Elec. 43 (1999) 1655.
[8] J.J. Fermé, Optical contacting, in: C. Amra, N. Kaiser, H.A. Macleod (Eds.), Optical Fabrication, Testing and Metrology, Proc. SPIE 5252 (2003) 26.
[9] J. Haisma, B. Spierings, U. Bierman, A. Van Gorkum, Appl. Opt. 33 (1994) 1154.
[10] A. Plössl, G. Kraüter, Mat. Sci. Eng. R25 (1999) 1.
[11] Q.-Y. Tong, Mat. Sci. Eng. B87 (2001) 323.
[12] L. Abel-Tibérini, F. Lemarquis, M. Lequime, Dedicated spectrophotometer for localized transmittance and reflectance measurements, in: Proceedings of Optical Interference Coatings, Tucson, 2004.
[13] J. Lumeau, Application de la photosensibilitéà la réalisation de filtres optiques interférentiels, PhD Thesis, Université Paul Cezanne Aix-Marseille III, 2004.